Carbohydrate Polymers 79 (2010) 620–627

Contents lists available at ScienceDirect

Carbohydrate Polymers

journal homepage: www.elsevier.com/locate/carbpol

Injectable hydrogels based on chitosan derivative/polyethylene glycol dimethacrylate/*N*,*N*-dimethylacrylamide as bone tissue engineering matrix

Guiping Ma [a], Dongzhi Yang [a], Qianzhu Li [a], Kemin Wang [a], Binling Chen [a], John F. Kennedy [b,*], Jun Nie [a,*]

[a] State Key Laboratory of Chemical Resource Engineering, Beijing University of Chemical Technology, Beijing 100029, PR China
[b] Chembiotech Laboratories, University of Birmingham Research Park, Vincent Drive, Birmingham B15 2SQ, UK

ARTICLE INFO

Article history:
Received 2 August 2009
Received in revised form 1 September 2009
Accepted 11 September 2009
Available online 18 September 2009

Keywords:
Chitosan
Hydrogel
Photopolymerization
Injectable

ABSTRACT

Injectable hydrogels were prepared from chitosan derivative (EGAMA-CS)/polyethylene glycol dimethacrylate (PEGDA)/*N*,*N*-dimethylacrylamide (DMMA) by photopolymerization. The morphology of the hydrogels was observed by scanning electron microscope (SEM). The relationship of double bond conversion with photopolymerization time was revealed by Real-time FTIR. The thermal behaviour of the hydrogels was investigated by differential scanning calorimetry (DSC), thermogravimetric analysis (TGA) and dynamic mechanical analysis (DMA). The equilibrium swelling ratio was also evaluated. In addition, the potential use of the hydrogels as scaffolding materials for bone regeneration was evaluated in vitro with Human bone sarcoma cell (SW1353) as reference cell lines. Indirect cytotoxicity assessment of the hydrogels indicated that the EGAMA-CS/PEGDA/DMMA hydrogels was non-toxic to the SW1353 cell. Cell culture results showed that fibrous mats were good in promoting the cell attachment and proliferation. The photopolymerized hydrogels are promised for the applications in the biomaterials area as bone tissue engineering matrix.

1. Introduction

Hydrogels are cross-linked, hydrophilic, and polymeric networks which could adsorb large amounts of water or biological fluids without dissolution. Hydrogels have been extensively used in the fields of biomedical and pharmaceutical engineering such as biosensors (Lee et al., 2008), membranes (Tokarev & Minko, 2009), artificial organs (Dai & Barbari, 2000), carriers for controlled drug delivery (Baljit et al., 2007; Murdan, 2003), and tissue engineering (Tan et al., 2009) because they are soft and rubbery, resembling a living tissue, biocompatibility, and biodegradability in the swollen state. Due to their similar physical properties to human tissues and their excellent tissue compatibility, hydrogels have been studied especially for biomedical applications (Berger et al., 2004; VanTomme et al., 2008). Most hydrogels were prepared via different technologies such as thermal polymerization (Huang et al., 1997) frontal copolymerization (Yan et al., 2005), radical copolymerization (Yue et al., 2009), graft copolymerization (Chung et al., 2005; Mahdavinia et al., 2004), γ-ray radiation-induced cross-linking (Wang et al., 2008; Yang et al., 2008), Non-covalent cross-linking (Marínez-Ruvalcaba et al., 2007), ionizing radiation (El-Rehim et al., 2006), redox polymerization (Yıldız et al., 2001), and photopolymerization (He et al., 2006; Jeon et al., 2009; Kytai & Jennifer, 2002).

Photopolymerized hydrogels have recently gained increased attention in biomedical applications because aqueous macromer solutions can be delivered in a minimally invasive manner and then photocrosslinked rapidly within few seconds in physiological conditions in situ following brief exposure to ultraviolet (UV) light (Schmedlen et al., 2002; Stalling et al., 2009). UV-photopolymerization is the most commonly applied method due to its distinct advantages of rapid cure, low curing temperature, in-line production, and low energy requirement (Marco et al., 2006). Photopolymerization is favored because hydrogels can be synthesized at temperatures and pH conditions near physiological conditions and even in the presence of biologically active materials. Furthermore, photopolymerization can be easily controlled by adjusting the dosage and intensity of UV light and the curing temperature. Numerous works have been published on the hydrogels based chitosan and their applications in the field of biomaterials in our research group (Han et al., 2009; Li et al., 2009; Zhou et al., 2008, 2009).

It is well accepted that natural polymers have better biocompatibility and less latent toxic effect than most synthetic polymers, pure natural polymer based hydrogels would be more suitable for application in biomedical fields. In recent years, hydrogels made of chitosan and chitosan derivatives have been investigated as skin regeneration (Nadège et al., 2007), drug release (Liu et al., 2008), and human osteoblasts (Lahiji et al., 2000) for its superior properties.

* Corresponding authors. Tel./fax: +86 01064421310.
E-mail address: niejun@mail.buct.edu.cn (J. Nie).

0144-8617/$ - see front matter © 2009 Published by Elsevier Ltd.
doi:10.1016/j.carbpol.2009.09.015

Chitosan is a cationic linear polysaccharide usually obtained by alkaline deacetylation of crustacean chitin from crab and shrimp shell wastes. Chitosan has been widely applied in drug delivery, gene therapy and tissue engineering because of its biocompatibility non-toxicity, antibacterial activity, biodegradability and many other superior properties. However, its poor solubility in physiological solvents and in common organic solvents due to its strong intermolecular hydrogen bonding, thereby greatly limited its biomedical applications, particularly as an injectable scaffold. The acidic solubility and the available gelation methods largely limited its application as an injectable hydrogel for tissue regeneration in vivo. Photopolymerization could overcome these problems, it could use in the fields of biological materials, and their physical properties are similar to human tissues.

The aim of this paper was to prepare EGAMA-CS/PEGDMA/DMMA composite hydrogels via photopolymerization. The relationship of double bond conversion of the hydrogels with the irradiation time of photopolymerization was revealed by Real-time FTIR. The intermolecular interaction and morphological change of the hydrogels were characterized by thermogravimetric analysis (TGA) and scanning electron microscope (SEM). The water states in swollen hydrogels were evaluated by differential scanning calorimetry (DSC). The swelling properties were investigated by measuring the equilibrium swelling ratios in distilled water. The potential use of this photopolymerized hydrogels as bone tissue engineering matrix material was evaluated in vitro with Human bone sarcoma cell (SW1353). The indirect cytotoxicity, cell adhesion, and cell proliferation were investigated as well.

2. Materials and methods

2.1. Materials

N,*N*-Dimethylacrylamide (DMMA) was obtained from Alfa Aesar (Tianjing China), Methacryloyloxy ethyl carboxyethyl chitosan (EGAMA-CS) was synthesized according to our previous report (Li et al., 2009), Polyethylene glycol (600) diacrylate (PEGDA600) was donated by Sarcomas Company (Warrington, PA, USA) and used without further purification. Photoinitiator 2959 (Darocur 2959, 2-hydroxy-1-[4-(hydroxyethoxy)phenyl]-2-methyl-1-propanone) was supplied from Ciba-Geigy Chemical Co. (Tom River, NJ). Human bone sarcoma cell (SW1353) was offered by Department of Microbiology, Peking University Health Science Center. All other reagents and solvents were purchased from Beijing Chemical Reagent Company (Beijing, China) and used without further purification.

2.2. Preparation of hydrogel by photopolymerization

Methacryloyloxy ethyl carboxyethyl chitosan (EGAMA-CS) solution (5 wt%) was prepared by dissolving EGAMA-CS powders in the distilled water at room temperature under constant stirring. Appropriate amounts N,N-dimethylacrylamide (DMMA), polyethylene glycol (600) diacrylate (PEGDA600), and photoinitiator 2959 was added to get the different weight ratio solutions.

The different weight ratio mixed solution was injected into a round mold consisting of two glass microslides separated by a spacer. The solution was irradiated with UV light source (30 mW/cm^2, 320–480 nm, EXFO lite, EFOS Corporation, Mississauga, Canada) for 15 min to form hydrogel. After the photopolymerization, the resultant hydrogels were immerged into the deionized water in order to remove the unreacted monomers and cut into circular pieces. The obtained hydrogel had a thickness of 2 mm and a diameter of 1.5 cm.

2.3. Characterization methods

2.3.1. Real-time FTIR

Real-time FTIR with a horizontal sample holder (Nicolet 5700, Thermo Electron, USA, equipped with an extended range KBr beam splitter and an MCT/A detector) was used to monitor the extent of polymerization. UV-photopolymerization triggered by EFOS Lite spot light source (5 mm crystal optical fiber, Canada) with 320–480 nm filter. The UV light intensity was 42 mW/cm^2 (Honle UV meter, Germany). The solutions were injected into a mold made from glass slides and spacers with 1.5 mm in diameter and 1.2 mm in thickness. Photopolymerizations were carried out at room temperature with the mixture of monomer and initiator. Real-time FTIR data were collected with resolution of 4 cm^{-1} and 0.3985 s sampling interval. The absorbance changes of the C=C peaks area from 6140 to 6210 cm^{-1} were correlated to the extent of photopolymerization (Decker & Moussa, 1989; Shi et al., 2007).

2.3.2. Scanning electron microscopy (SEM)

Morphologies and pore structures of composite hydrogels were characterized on a Hitachi S-4700 Scanning electron microscope (Hitachi company, Japan) at an accelerating voltage of 20 kV. Prior to the observation, specimen was immersed into liquid nitrogen, fractured, and then sputtered with a thin layer of gold.

2.3.3. Differential scanning calorimetry (DSC)

Differential scanning calorimetry (DSC 204 F1, Netzsch, Germany) was performed to evaluate the state of water in the swollen hydrogels and T_g. The experiments were performed as follows, 25 mg samples were sealed in aluminum pans, cooled down to −100 °C at the rate of 10 °C/min, and then heated to 150 °C at the rate of 10 °C/min. The open aluminum cell was swept with N_2 at 20 mL/min during the analysis.

2.3.4. Thermal-gravimetric analysis (TGA)

Thermal-gravimetric analysis (TGA) was carried out with a netzsch TG 209 C Iris system (Germany). The analysis was performed with a 5 mg sample in aluminum pans under a dynamic nitrogen atmosphere between 30 and 500 °C, and the experiment was run at rate of 10 °C/min.

2.3.5. Equilibrium swelling ratio

The known weights of freeze-dried hydrogels were immersed in distilled water, and at appropriate time intervals, the hydrogels were taken out. The swollen hydrogels were immediately weighed with a microbalance after the excess of water lying on the surfaces was absorbed with a filter paper. The swollen masses of the hydrogels were then compared with their dry masses in order to calculate the equilibrium swelling ratio (SR) according to the following equation (Tan et al., 2009).

$$SR = (W_s - W_d)/W_d$$

where W_s and W_d are the weights of the hydrogels at the equilibrium swelling state and the dried state, respectively.

2.3.6. Dynamic mechanical analyzer (DMA)

A dynamic mechanical analyzer (DMA) (Rheometyic, USA) was used to perform the mechanical properties measurement. The polymerized samples were kept at room temperature for 120 h after curing to ensure that post-polymerization process was completed. The samples used for DMA were thin rectangular films of approximately 1.2 mm thickness and dimensions of 7 mm × 35 mm. Dynamic mechanical analysis was performed over a temperature range from −25 °C to 75 °C with a ramping rate of 5 °C per minute. The loss and storage modulus and the loss tangent (tan δ, ratio of loss to storage modulus) were recorded as a function

of temperature, and the glass transition temperature (T_g) was taken to be the maximum of the loss tangent vs. temperature curve.

2.3.7. Methylthiazolydiphenyl-tetrazolium bromide (MTT) assay

MTT (3-[4,-dimethylthiazol-2-yl]-2,5-diphenyltetrazolium bromide; thiazolyl blue) assay was performed according to our reports (Han et al., 2009; Zhou et al., 2009) for detecting toxic products or adverse reactions, which could be evaluated through in vitro cytotoxic tests. With a standard as ISO10993-5 test method, the prepared blend films were sterilized with highly compressed steam for 15 min and placed in extraction media (RPMI1640, 10% fetal bovine serum, 1.0% penicillin–streptomycin, 1.2% glutamine), respectively, and steeped at 37 °C for 24 h. The extraction ratio was 0.15 g/mL. Then the blend films were removed and the extracts were stored for evaluation of cytotoxicity. Human bone sarcoma cell (SW1353), which was cultured with the extraction media in comparison with control. Culture was maintained at 37 °C in a wet atmosphere. When the cells reached 80% confluence, they were trypsinized with 0.25% trypsin containing 1 mM ethylenediamine tetraacetic acid (EDTA). MTT reagent is a yellow tetrazolium salt that produces a dark-blue formazan crystal when incubated with viable cells. Therefore, the level of the reduction of MTT into formazan can reflect the level of cell metabolism.

SW1353 cells were seeded in wells of a 96-well plate at a density of 10^3 cells per well. After incubation for 24 h, the culture medium was removed and replaced with the as-prepared extraction media. After incubated for 24, 48, 72 h, each well was taken out, and 100 μL MTT solution was added to each well. After incubated for 4 h at 37 °C, 150 μL of dimethyl sulfoxide was added to dissolve the formazan crystals. The dissolved solution was swirled homogeneously about 10 min by the shaker. The optical density of the formazan solution was detected by an ELISA reader (Multiscan MK3, Labsystem Co., Finland) at 570 nm. For reference purposes, cells were seeded in a fresh culture medium (negative control) under the same seeding conditions, respectively. Each assay was performed six times.

2.3.8. Cell culture and adhesion

The prepared hydrogels with 1.5 cm in diameter, stated on glass coverslips using cooper tape, were sterilized with highly compressed steam for 15 min. Then the hydrogels were extensively washed three times with sterile phosphate buffered saline (PBS) and transferred to individual 24-well tissue culture plates. Aliquots (1 mL) of SW1353 suspension with 1.5×10^4 cell/mL were seeded on the sample membranes. After 48 h of culture, cellular constructs were harvested, rinsed twice with PBS to remove non-adherent cells and subsequently fixed with 3.0% glutaraldehyde at 4 °C for 4 h. After that, the samples were dehydrated through a series of graded ethanol solutions and air-dried overnight. Dry samples were sputtered with gold for observation of cell morphology on the surface of the scaffolds by SEM.

3. Results and discussion

3.1. Real-time FTIR

The bond conversion double vs. irradiation time of photopolymeried hydrogels with different weight ratio is shown in Fig. 1. When irradiated under UV light with 2959 as photoinitiator, the C═C double bond of EGAMA-CS, PEGDMA, and DMMA start to copolymerize and the area of C═C double bond absorbance peak near 6140–6210 cm^{-1} decreased or disappeared in Real-time FTIR. The different composite hydrogels all have the high photopolymerization rate and final double bond conversion. But increase the concentration of EGAMA-CS of favorable the polymerization rate

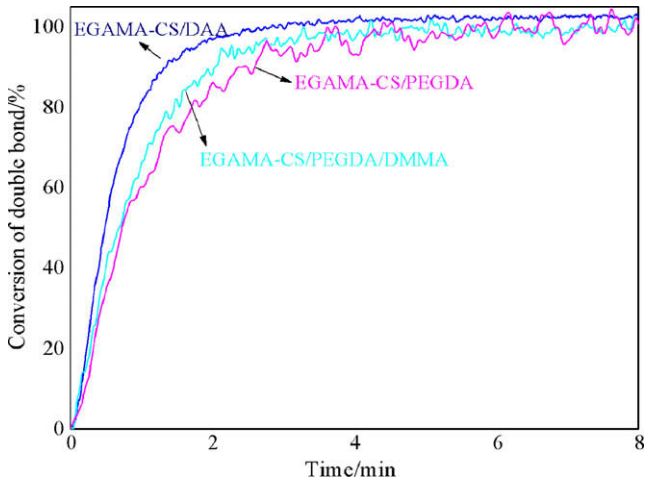

Fig. 1. Conversion double bond of vs. irradiation time of photopolymerized hydrogels with different weight ratio.

and final double bond conversion. The conversion of C═C double bond of polymerization of EGAMA-CS/DMMA hydrogel could lead to high ratio within few minutes and final double bond conversion could reach 98% within 3 min. The higher concentration of double bond of per unit, and the higher conversion double bond rate. PEG-

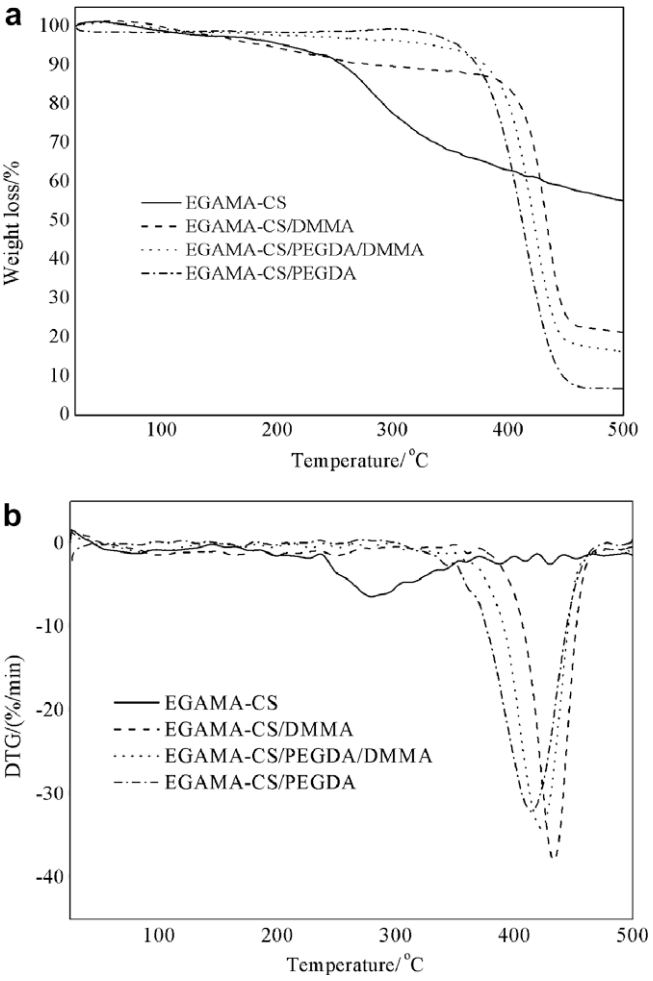

Fig. 2. TG thermograms (a) and DTG curves (b) of photopolymerized EGAMA-CS/PEGDMA/DMMA hydrogels.

DA is high-molecular compound contained the flexible ethylene glycol chain with two double bonds at the ends of chain, and its concentration of double bond of per unit was lower than that of DMMA during the photopolymerization.

3.2. Thermal-gravimetric analysis

The TGA result of photopolymerized hydrogels is displayed in Fig. 2. PEGDA-CS showed its thermal degradation in two stages. The first range of moderate thermal decomposition from the beginning of the temperature to 120 °C with a weight loss of 8% ascribed to the volatile low molecular products and water. The second decomposition stage of PEGDA-CS started at 235 °C till 445 °C and reached the maximum at 280 °C, with weight loss of 45%. This phase of the weight loss mainly caused by a series of complex chemical changes in the process including the sugar ring dehydration, degradation, molecular chain acetaminophen and N-deacetylation of the cracking unit. The photopolymerized EGAMA-CS/DMMA hydrogel showed the obvious degradation between 270 °C and 460 °C, with the maximum decomposition rate at about 430 °C and weight loss of 78%, which attributed to the decomposition of DMMA and EGAMA-CS. The EGAMA-CS/PEGDA photopolymerized hydrogel showed the obvious degradation between 330 °C and 450 °C, with the maximum decomposition rate at about 415 °C and weight loss of 92%, which owed to the decomposition of PEGDA and EGAMA-CS. It could indicate that thermal stability of the photopolymerized hydrogel was less than that of chitosan and more stable than PEGDMA and DMMA due to weakening of inter- and extra-molecular hydrogen bonding.

3.3. Differential scanning calorimetry (DSC)

DSC spectra of photopolymerized hydrogels are shown in Fig. 3. The content of different water state (free water or bond water) in swollen hydrogels was investigated from the DSC melting thermograms of swollen hydrogels. The endothermic peaks of hydrogels at about 3 °C due to free water, which could be calculated as the ratio of endothermic peak areas between 0 and 6 °C for water of swollen hydrogels to melting endothermic heat of pure water. The endothermic peaks at about 25–95 °C in the spectra of the hydrogels assigned to the hydrogen bonding was determined by the total water and free water. With the combination of the equilibrium swelling ratio of the hydrogels, the free water and bond water contents of the EGAMA-CS/DMMA, EGAMA-CS/PEGDA and EGAMA-CS/PEGDA/DMMA hydrogels were 84.3% and 9.8%, 17.7% and 48.9%, 32.5% and 50.8%, respectively. The photopolymerized EGAMA-CS/DMMA hydrogel has the high ability of water absorption because DMMA formed the low cross-linking density in the hydrogel which could absorb much water. The ability of water absorption of photopolymerized EGAMA-CS/PEGDA hydrogel was lower than that of EGAMA-CS/DMMA hydrogel due to PEGDA could form high dense network structure.

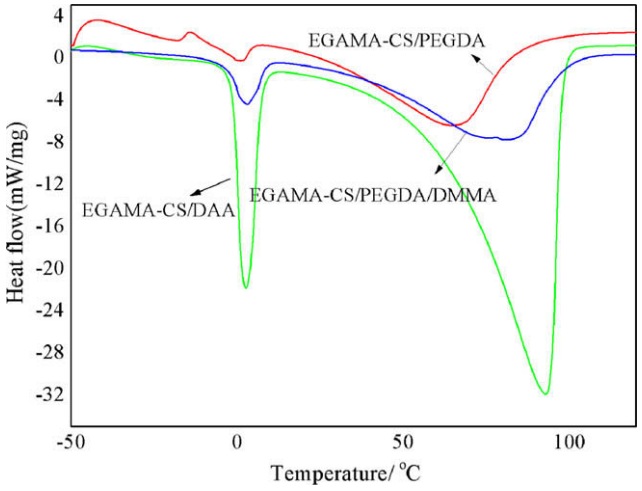

Fig. 3. DSC curves of photopolymerized hydrogels.

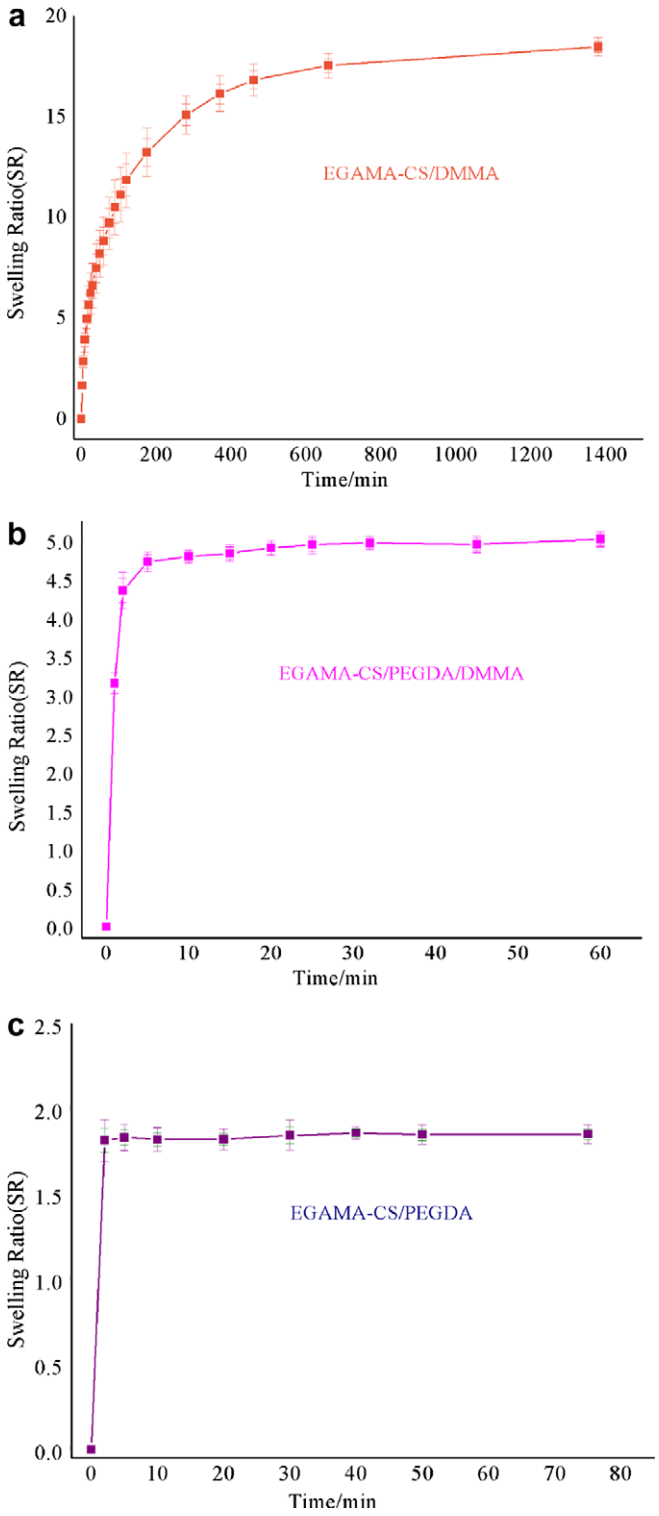

Fig. 4. Equilibrium swelling ratio of freeze-dried photopolymerized EGAMA-CS/PEGDMA/DMMA hydrogels in distilled water.

3.4. Equilibrium swelling ratio

Fig. 4 indicates the equilibrium swelling ratio of freeze-dried photopolymerized hydrogels. Regarding the kinetic's profile of the equilibrium swelling process in Fig. 4a, the photopolymerized hydrogels reached the equilibrium swelling ratio in long time, and the equilibrium swelling ratio index was high. It was understandable by the water gradual diffusion into the polymer core. The swelling ratio was increased along with increase content of EGAMA-CS. The higher ionization of the amine groups and the high volume acetyl groups in the EGAMA-CS chains was responsible for the chain expansion, thus allowing a higher degree of equilibrium swelling ratio (Santos et al., 2006). However, in Fig. 4b its swelling kinetics approached a typical rectangular hyperbolic function. The equilibrium swelling ratio index was low and the maximum swelling ratio was reached balance almost instantly and. It indicated that the incorporation of PEGDA, a more hydrophilic monomer in the formulation resulted in the weaker water capacity and lower equilibrium swelling ratio (Ng & Swami, 2005).

3.5. Morphologies of hydrogels

SEM images were obtained to characterize the microstructure morphologies of three freeze-dried photopolymerized hydrogels in Fig. 5. It could be seen that the inner pores of the hydrogels were interconnected with irregular shapes, the pore sizes ranging from 20 to 110 μm throughout the lyophilized hydrogel, and the number of pore increased with the increase of the concentration of PEGDA in the hydrogels. The internal morphology was dependent on the content of EGAMA-CS, and the higher ratio of EGAMA-CS resulted in the smaller pore sizes. This could be understandable since the solid content (EGAMA-CS) was 6 wt% and freeze-drying generally created a scaffold with open pore morphology (Hong et al., 2007). Samples showed the co-continuous or interconnect open porous structure, which showed that PEGDA as a scaffold responsible for the framework of the final product (Park et al., 2009). The porous structure was favor to the cell adhesion and profiltion.

3.6. Dynamic mechanical behaviour

The mechanical properties of the scaffold are key determinants of its long-term success or eventual failure and influence the mechanical environment of the profiled cells when it is implanted into an osteochondral defect (Malafaya & Reis, 2009). The different frequency (1, 2, 5 and 10 Hz) of the storage modulus and the loss factor of photopolymerized hydrogels are shown in Fig. 6. The scaffolds showed excellent mechanical behaviour when compared to the typical mechanical properties obtained for chitosan-based porous materials (Malafaya et al., 2008). The variation of storage modulus E′ was quite similar with the trend displayed and increased with increase frequency for the system of EGAMA-CS/DMMA hydrogels. The storage modulus E′ of EGAMA-CS/DMMA hydrogels

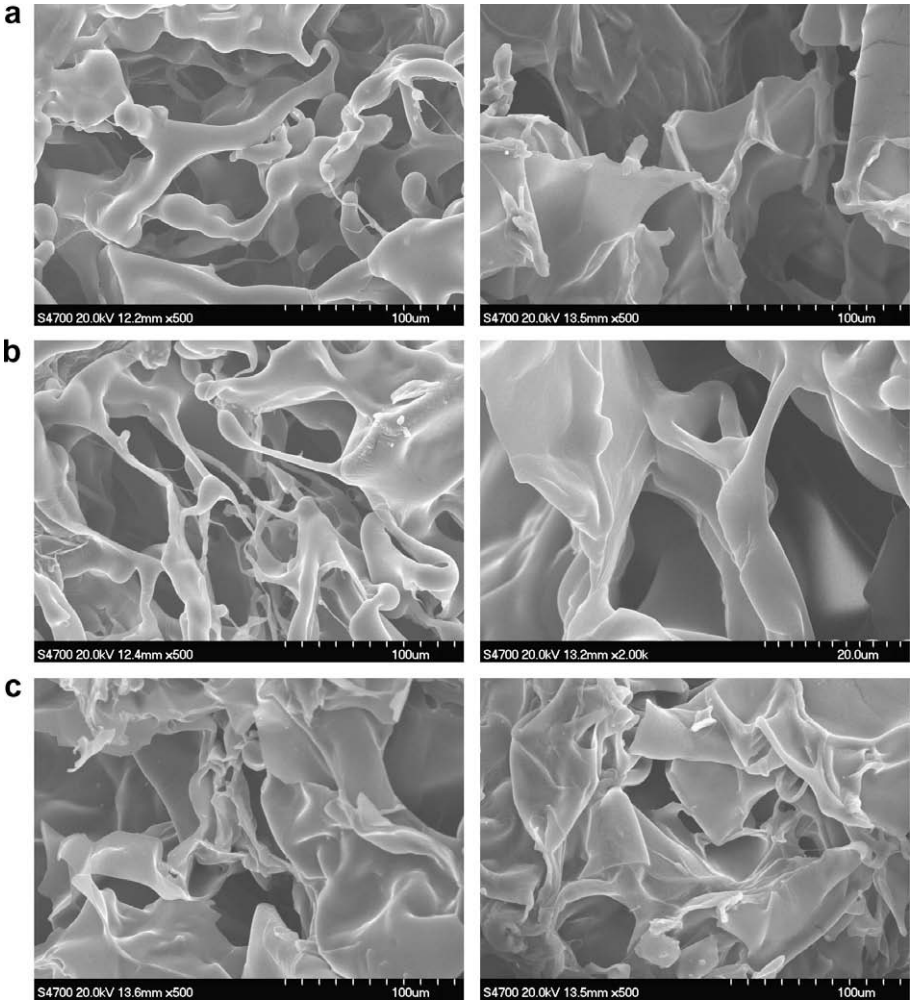

Fig. 5. SEM micrographs of photopolymerized EGAMA-CS/PEGDMA/DMMA hydrogels.

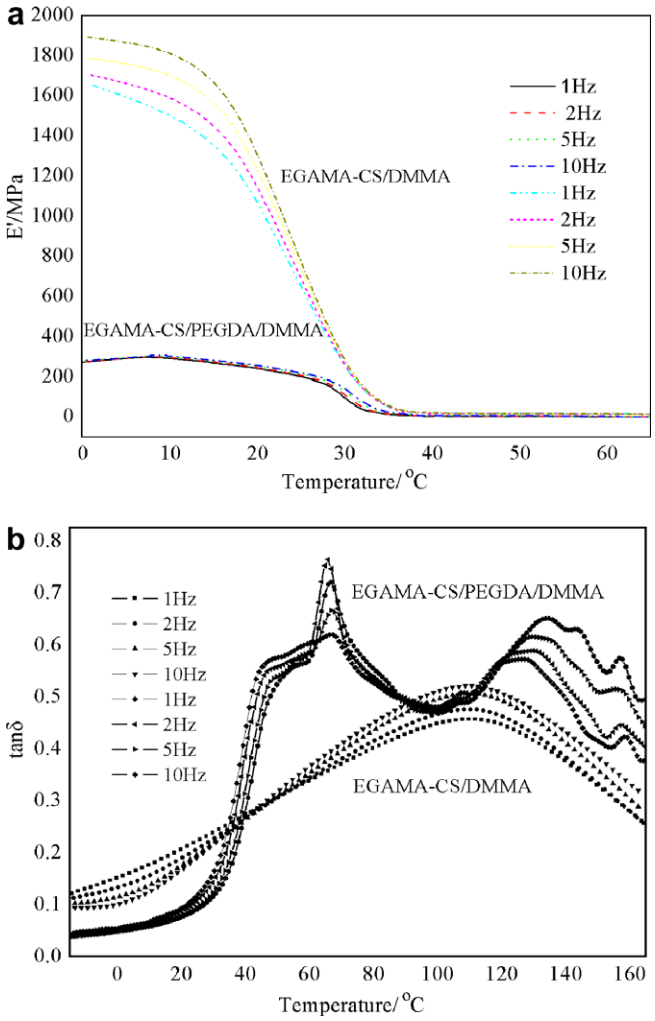

Fig. 6. Storage modulus (E′) (a) and loss factor (tan δ) (b) as a function of temperature for photopolymerized EGAMA-CS/PEGDMA/DMMA hydrogels measured by DMA.

was higher than that of EGAMA-CS/PEGDA/DMMA hydrogels due to the high-molecular PEGDA. The tan δ also presented a well defined peak around 108 °C and reached high values at 110 °C, and the peak was shifted towards higher temperature with increase frequency. For the system of EGAMA-CS/PEGDA/DMMA, the temperature corresponding to the maximum of the peaks in the plot of tan δ were assumed to be the relaxation temperature, glass transition (T_g) or secondary relaxation. The sharp peak at 62 °C was associated with the glass transition temperature, and the broader relaxation with maximum at 138 °C which was attributed to secondary dispersion (Katarzyna, 2009; Sun et al., 2008).

3.7. Methylthiazolydiphenyl-tetrazolium bromide (MTT) assay

Toxicity test is an important aspect of biomaterials. An ideal tissue engineer material should not release toxic products or produce adverse reactions, which could be evaluated through in vitro cytotoxic tests. Fig. 7 shows the absorbance of sample (EGAMA-CS/PEGDA/DMMA, EGAMA-CS/PEGDA) obtained from an MTT assay of SW1353 which were cultured with the extraction media from various types of specimens. It could be seen that, no statistically significant differences ($p < 0.05$) were observed in the cell activity within 72 h in the presence of hydrogels extracts in comparison with negative control although the average absorbance values were lower than that of the control condition. We could also conclude that the biocompatibility of photopolymerized EGAMA-CS/PEGDA/DMMA hydrogels was higher than that of photopolymerized EGAMA-CS/PEGDA hydrogels. It would conclude that photocrosslinked hydrogels sample of EGAMA-CS/PEGDA/DMMA was thought non-toxic to SW1353.

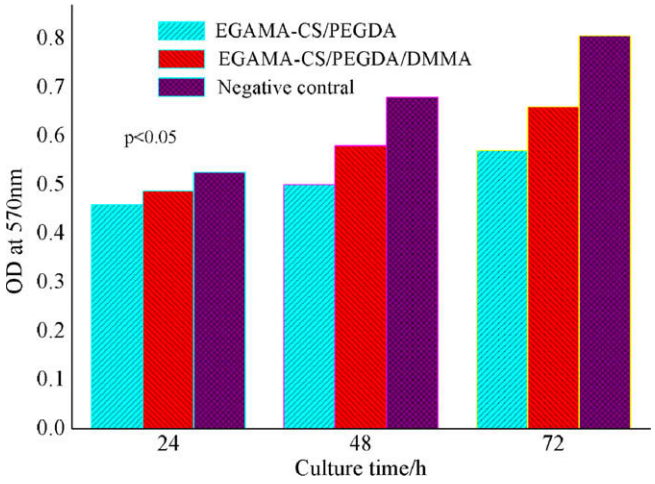

Fig. 7. Cytotoxicity test of photopolymerized EGAMA-CS/PEGDMA/DMMA hydrogels with positive and negative controls ($p < 0.05$) $^{*}p < 0.05$ when compared to the negative control of indirect cytotoxicity. The data represented mean and standard deviations of six samples.

3.8. Cell adhesion and morphology

SW1353 cell was conducted by indirect cytotoxicity in order to examine the interaction of the hydrogel with tissue cells, and the cells test was operated according to the ISO10993-5 standard test method. The SEM morphologies of the adhered SW1353 cells after 48 h of culture on the surfaces of photopolymerized cross-linked hydrogels are shown in Fig. 8. After 48 h of culture, the majority of the cells were attached and spread on the surface of hydrogel, and exhibited a normal morphology on the surface which was due to the large surface area available for cell attachment and proliferation (Zhou et al., 2009). It also showed that cells were flattened and exhibited short and numerous microvilli on the etched surface of hydrogels (Coutinho et al., 2008). The results suggested that EGAMA-CS/PEGDA/DMMA hydrogel was suite for the adhesion, spreading, and proliferation of SW1353 and it could be candidate as bone tissue engineering matrix.

4. Conclusion

The EGAMA-CS/PEGDMA/DMMA hydrogels was successfully prepared by photopolymerization technology and the thermal behaviour was characterized in terms of DMA, DSC, and TGA. The structure of the hydrogels was analyzed by SEM. The hydrogel could lead to high ratio within few minutes and final double bond conversion could reach 98%. The photopolymerized hydrogels have the strong ability of absorb water in distilled water, showed excellent mechanical behaviour, and had the good thermal stability. Indirect cytotoxicity assessment of photopolymerized hydrogels with Human bone sarcoma cell (SW1353) indicated that the material showed no cytotoxicity toward growth of SW1353 cell and had good in vitro biocompatibility. Cell culture suggested that the photopolymerized hydrogels did well at promoting cell adhesion and proliferation. These novel photopolymerized hydrogels have the potential to be used as materials for bone tissue engineering matrix.

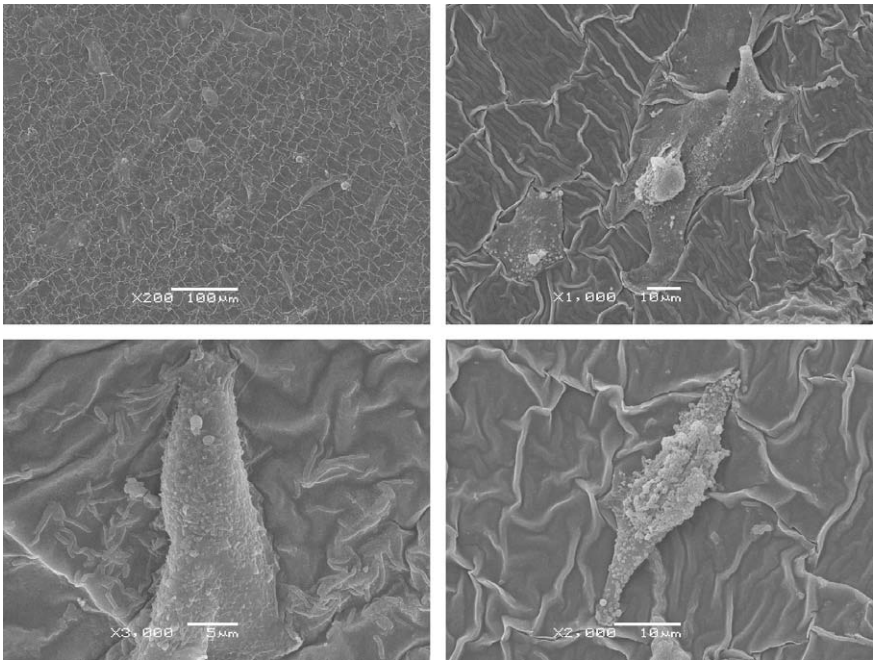

Fig. 8. SEM images of SW1353 cell seeded on photopolymerized hydrogels membrane of EGAMA-CS/PEGDMA/DMMA after 48 h culture.

Acknowledgements

The author would like to thank the National Natural Science Foundation of China (50803004) for its financial support. This study was supported by the Program for Changjiang Scholars and Innovative Research Team in University and Open Fund from Key Laboratory of Beijing City on Preparation and Processing of Novel Polymer Materials, Beijing University of Chemical Technology.

References

Baljit, S. et al. (2007). Synthesis, characterization and swelling studies of pH responsive psyllium and methacrylamide based hydrogels for the use in colon specific drug delivery. *Carbohydrate Polymers, 69*, 631–643.

Berger, J. et al. (2004). Structure and interactions in chitosan hydrogels formed by complexation or aggregation for biomedical applications. *European Journal of Pharmaceutics and Biopharmaceutics, 57*, 35–52.

Chung, H. J. et al. (2005). Thermosensitive chitosans as novel injectable biomaterials. *Macromolecular Symposia, 224*, 275–286.

Coutinho, D. F. et al. (2008). The effect of chitosan on the in vitro biological performance of chitosan-poly(butylene succinate) blends. *Biomacromolecules, 9*, 1139–1145.

Dai, W. S., & Barbari, T. A. (2000). Gel-impregnated pore membranes with mesh-size asymmetry for biohybrid artificial organs. *Biomaterials, 21*, 1363–1371.

Decker, C., & Moussa, K. (1989). Real-time kinetic study of laser-induced polymerization. *Macromolecules, 22*, 4455–4462.

El-Rehim, H. A. et al. (2006). Effect of various environmental conditions on the swelling property of PAAm/PAAcK superabsorbent hydrogel prepared by ionizing radiation. *Journal Applied of Polymer Science, 101*, 3955–3962.

Han, J. et al. (2009). Photopolymerization of methacrylated chitosan/PNIPAAm hybrid dual-sensitive hydrogels as carrier for drug delivery. *International Journal of Biological Macromolecules, 44*, 229–235.

He, H. Y. et al. (2006). Photopolymerization and structure formation of methacrylic acid based hydrogels in water/ethanol mixture. *Polymer, 47*, 1612–1619.

Hong, Y. et al. (2007). Covalently crosslinked chitosan hydrogel: Properties of in vitro degradation and chondrocyte encapsulation. *Acta Biomaterialia, 3*, 23–31.

Huang, C. W. et al. (1997). Curing kinetics of the synthesis of poly(2-hydroxyethyl methacrylate) (PHEMA) with ethylene glycol dimethacrylate (EGDMA) as a crosslinking agent. *Journal of Polymer Science Part A: Polymer Chemistry, 35*, 1873–1889.

Jeon, O. et al. (2009). Photocrosslinked alginate hydrogels with tunable biodegradation rates and mechanical properties. *Biomaterials, 30*, 2724–2734.

Katarzyna, L. D. (2009). Miscibility and thermal stability of poly(vinyl alcohol)/chitosan mixtures. *Thermochimica Acta, 493*, 42–48.

Kytai, T. N., & Jennifer, L. W. (2002). Photopolymerizable hydrogels for tissue engineering applications. *Biomaterials, 23*, 4307–4314.

Lahiji, A. et al. (2000). Chitosan supports the expression of extracellular matrix proteins in human osteoblasts and chondrocytes. *Journal of Biomedical Materials Research, 51*, 586–595.

Lee, W. et al. (2008). Preparation of micropatterned hydrogel substrate via surface graft polymerization combined with photolithography for biosensor application. *Sensors and Actuators B: Chemical, 129*, 841–849.

Li, Q. Z. et al. (2009). Synthesis and characterization of chitosan-based hydrogels. *International Journal of Biological Macromolecules, 44*, 121–127.

Liu, K. H. et al. (2008). Drug release behavior of chitosan–montmorillonite nanocomposite hydrogels following electrostimulation. *Acta Biomaterialia, 4*, 1038–1045.

Mahdavinia, G. R. et al. (2004). Modified chitosan III, superabsorbency, salt- and pH-sensitivity of smart ampholytic hydrogels from chitosan-g-PAN. *Polymers for Advanced Technologies, 15*, 173–180.

Malafaya, P. B. et al. (2008). Morphology, mechanical characterization and in vivo neo-vascularization of chitosan particle aggregated scaffolds architectures. *Biomaterials, 29*, 3914–3926.

Malafaya, P. B., & Reis, R. L. (2009). Bilayered chitosan-based scaffolds for osteochondral tissue engineering: Influence of hydroxyapatite on in vitro cytotoxicity and dynamic bioactivity studies in a specific double-chamber bioreactor. *Acta Biomaterialia, 5*, 644–660.

Marco, S. et al. (2006). Synthesis and cationic photopolymerization of new fluorinated, polyfunctional propenyl ether oligomers. *Journal of Polymer Science Part A: Polymer Chemistry, 44*, 6943–6951.

Marŕnez-Ruvalcaba, A. et al. (2007). Viscoelastic properties of dispersed chitosan/xanthan hydrogels. *Carbohydrate Polymers, 67*, 586–595.

Murdan, S. (2003). Electro-responsive drug delivery from hydrogels. *Journal of Controlled Release, 92*, 1–17.

Nadège, B. et al. (2007). The use of physical hydrogels of chitosan for skin regeneration following third-degree burns. *Biomaterials, 28*, 3478–3488.

Ng, L. T., & Swami, S. (2005). IPNs based on chitosan with NVP and NVP/HEMA synthesized through photoinitiator-free photopolymerisation technique for biomedical applications. *Carbohydrate Polymers, 60*, 523–528.

Park, K. M. et al. (2009). Thermosensitive chitosan-pluronic hydrogel as an injectable cell delivery carrier for cartilage regeneration. *Acta Biomaterialia, 5*, 1956–1965.

Santos, C. et al. (2006). Acetylation and molecular mass effects on barrier and mechanical properties of shortfin squid chitosan membranes. *European Polymer Journal, 42*, 3277–3285.

Schmedlen, R. H. et al. (2002). Photocrosslinkable polyvinyl alcohol hydrogels that can be modified with cell adhesion peptides for use in tissue engineering. *Biomaterials, 23*, 4325–4332.

Shi, S. Q. et al. (2007). Cyclic acetal as coinitiator for bimolecular photoinitiating systems. *Polymer, 48*, 2860–2865.

Stalling, S. S. et al. (2009). Development of photocrosslinked methylcellulose hydrogels for soft tissue reconstruction. *Acta Biomaterialia, 5*, 1911–1918.

Sun, H. L. et al. (2008). Surface-modified zeolite-filled chitosan membranes for pervaporation dehydration of ethanol. *Applied Surface Science, 254*, 5367–5374.

Tan, H. P. et al. (2009). Injectable in situ forming biodegradable chitosan–hyaluronic acid based hydrogels for cartilage tissue engineering. *Biomaterials, 30*, 2499–2506.

Tokarev, I., & Minko, S. (2009). Hierarchically structured membranes: New, challenging, biomimetic materials for biosensors, controlled release, biochemical gates, and nanoreactors. *Advanced Materials, 21*, 241–247.

VanTomme, S. R. et al. (2008). In situ gelling hydrogels for pharmaceutical and biomedical applications. *International Journal of Pharmaceutics, 355*, 1–18.

Wang, M. et al. (2008). Γ-ray radiation-induced synthesis and Fe(III) ion adsorption of carboxymethylated chitosan hydrogels. *Carbohydrate Polymers, 74*, 498–503.

Yan, Q. et al. (2005). Frontal copolymerization synthesis and property characterization of starch-graft-poly(acrylic acid) hydrogels. *Chemistry European Journal, 11*, 6609–6615.

Yang, X. M. et al. (2008). Investigation of PVA/ws-chitosan hydrogels prepared by combined γ-irradiation and freeze-thawing. *Carbohydrate Polymers, 73*, 401–408.

Yıldız, B. et al. (2001). Synthesis of thermoresponsive N-isopropylacrylamide–N-hydroxymethyl acrylamide hydrogels by redox polymerization. *Polymer, 42*, 2521–2529.

Yue, Y. et al. (2009). Fabrication and characterization of microstructure and pH sensitive interpenetrating networks hydrogel films and application in drug delivery field. *European Polymer Journal, 45*, 309–315.

Zhou, Y. Z. et al. (2008). A pH-sensitive water-soluble N-carboxyethyl chitosan/poly(hydroxyethyl methacrylate) hydrogel as a potential drug sustained release matrix prepared by photopolymerization technique. *Polymers for Advanced Technologies, 19*, 1133–1141.

Zhou, Y. S. et al. (2009). Semi-interpenetrating polymer network hydrogels based on water-soluble N-carboxylethyl chitosan and photopolymerized poly(2-hydroxyethyl methacrylate). *Carbohydrate Polymers, 75*, 293–298.